

Symmetry protected phases in inhomogeneous spin chains

Nadir Samos Sáenz de Buruaga¹, Silvia N. Santalla², Javier Rodríguez-Laguna³ and Germán Sierra¹

¹ Instituto de Física Teórica UAM/CSIC, Universidad Autónoma de Madrid, Cantoblanco, Madrid, Spain

² Dept. de Física and Grupo Interdisciplinar de Sistemas Complejos (GISC), Universidad Carlos III de Madrid, Spain

³ Dept. de Física Fundamental, Universidad Nacional de Educación a Distancia (UNED), Madrid, Spain

(Dated: February 1, 2022)

It has been shown recently that inhomogeneous spin chains can exhibit exotic phenomena such as the breaking of the area law of the entanglement entropy. An example is given by the rainbow model where the exchange coupling constants decrease from the center of the chain. Here we show that by folding the chain around its center, the long-range entanglement becomes short-range which can lead to topological phases protected by symmetries (SPT). The phases are trivial for bond-centered foldings, and non trivial for site-centered ones. In the latter case, the folded spin 1/2 chain with $U(1)$ symmetry belongs to the Su-Schrieffer-Heeger class, while the folded chain with $SU(2)$ symmetry is in the Haldane phase. Finally, we extend these results to higher spin chains where we find a correspondence between the symmetry protection of gapped and gapless phases.

Introduction.— In the last years, an area called Quantum Matter has emerged, where Condensed Matter Physics and Quantum Optics find a common ground to exchange ideas and techniques. Some antecedents of this area can be found in the 80's in the integer and fractional Quantum Hall effects [1] that paved the way to the more recent discovery of topological insulators and superconductors [2], Weyl semimetals [3], etc. The description of Quantum Matter goes beyond the Landau paradigm in terms of symmetry breaking and local order parameters. The fundamental concept here is that of topology which in this context means that the relevant properties of a physical system are distributed throughout its extent, whose characterization requires the use of advanced mathematical tools [4–20].

In this letter we shall focus on 1D spin systems whose topological properties have been characterized in various ways. Consider for example the antiferromagnetic Heisenberg chain (AFH) of spin 1. As famously conjectured by Haldane[21], the AFH Hamiltonian has a unique ground state which does not break the rotational symmetry $SO(3)$, and has a gap in the spectrum for periodic chains. This conjecture led Affleck et al. [22] to propose a state whose properties are similar to those of Haldane's state, and whose many-body wave function is a matrix product state (MPS) [23, 24]. The topological properties of the Haldane and the AKLT states were characterized by an string order parameter of den Nijs and Rommelse [25] or a symmetry dependent string order parameter [26], and the existence of effective spins 1/2 at the ends of an open chain. It was realized that the Haldane phase can be protected by several symmetries like $Z_2 \times Z_2$ [5], time reversal and inversion symmetry [7, 15], which guarantee *independently* the degeneracy of the entanglement spectrum. More importantly, the concept of symmetry protection turns out to be the key to understand and classify the phases with short range entanglement where one can apply the MPS techniques [12, 14].

Here we present a new way to generate symmetry pro-

tected phases in 1D using local Hamiltonians that are inhomogeneous and without a gap in the spectrum. At first glance, one does not expect this possibility to occur because the corresponding ground states would develop long-range entanglement that violates the area-law [27–29]. However, we will show that a rearrangement of the sites transforms the long-range entanglement into a short-range entanglement, where standard methods can be applied to identify the possible phases [14, 16]. The inhomogeneous models that we will consider are obtained by a deformation of the critical models where the entropy of entanglement scale logarithmically [30, 31]. The effect of the lack of homogeneity is to increase this violation that becomes linear in the size of the blocks, like a thermal entropy. This mechanism has a geometrical interpretation in the underlying conformal field, according to which inhomogeneity corresponds to a curvature of space-time [32, 33].

A byproduct of our construction is that it suggests a relationship between the SPT phases and the phases described by conformal field theories (CFT) in terms of global anomalies [20]. The reason is that the former are constructed from a special deformation of the latter. We shall illustrate this relation with several examples.

The rainbow XX model.— We start with the inhomogeneous XX spin chain whose exchange coupling constants decrease exponentially from the center [29, 32–36]. This model is equivalent to a spinless fermion model by a Jordan-Wigner transformation. The Hamiltonian for a closed chain with an even number of sites, $2L$, is

$$H = -\frac{1}{2} \sum_{n=1}^{2L} J_n c_n^\dagger c_{n+1} + h.c. \quad (1)$$

where c_n is the fermion annihilation operator, and $c_{2L+1} = c_1$. We define models with bond-centered symmetry (bcs) and site-centered symmetry (scs) as those satisfying

$$J_n = J_{2L-n} \text{ (bcs)}, \quad J_n = J_{2L+1-n} \text{ (scs)} \quad (2)$$

that correspond to inversions around bond $(L, L+1)$ and site $L+1$ respectively. The lack of homogeneity is introduced in terms of an exponential decrease of the hopping parameters from the center of the chain outwards,

$$J_{n \neq L} = e^{-h|n-L|}, \quad J_L = e^{-\frac{h}{2}} \quad (\text{bcs}), \quad (3)$$

$$J_{n \neq L, L+1} = e^{-h(|n-(L+\frac{1}{2})|-\frac{1}{2})}, \quad J_L = J_{L+1} = e^{-\frac{h}{2}} \quad (\text{scs}),$$

where $h \geq 0$ is the inhomogeneity parameter. The symmetries of the two types of chains are illustrated in Fig. 1. In the bcs model the highest coupling lies at the center of the chain, that is J_L , while the weakest coupling is $J_{2L} = e^{-hL}$ that connects sites 1 and $2L$. In the strong inhomogeneity limit $hL \gg 1$, one can set J_{2L} to zero which leads to the rainbow chain studied in references [32–36]. Using the Dasgupta-Ma RG method [37, 38] it was shown that the ground state of the rainbow chain takes the form [34]

$$|\text{bcs}\rangle \xrightarrow{h \rightarrow \infty} d_{+1}^\dagger d_{-2}^\dagger d_{+3}^\dagger \dots d_{\eta_L L}^\dagger |0\rangle, \quad (4)$$

where

$$d_{\pm n} = \frac{1}{\sqrt{2}}(c_{L+1-n} \pm c_{L+n}), \quad n = 1, \dots, L, \quad (5)$$

are fermion operators on the opposite sides of the chain, that annihilate the Fock vacuum $|0\rangle$ and $\eta_L = (-1)^{L+1}$. This state presents a maximal violation of the entanglement entropy for the block $A = \{1, 2, \dots, \ell\}$:

$$S_A^{\text{bcs}} = \ell \ln 2, \quad \ell \leq L. \quad (6)$$

Let us consider now chains with site-centered symmetry. In the limit $h \gg 1$, the dominant interaction takes place between sites $L, L+1$ and $L+2$. In this situation one should use first order perturbation theory to renormalize three spins into one effective spin (Supplementary Material). Iterating this RG procedure one obtains the ground state,

$$|\text{scs}\rangle \xrightarrow{h \rightarrow \infty} b_{+0}^\dagger b_{-1}^\dagger b_{+2}^\dagger b_{-3}^\dagger \dots b_{+L}^\dagger |0\rangle, \quad (7)$$

where

$$f_0 = c_{L+1}, \quad f_L = c_1 \quad (8)$$

$$f_{\pm n} = \frac{1}{\sqrt{2}}(c_{L+1-n} \pm c_{L+1+n}), \quad n = 1, \dots, L-1,$$

$$b_{\pm 0} = \frac{1}{\sqrt{2}}(f_0 \pm f_{+1}), \quad b_{\pm L} = \frac{1}{\sqrt{2}}(f_0 \pm f_{+L-1}),$$

$$b_{\pm n} = \frac{1}{\sqrt{2}}(f_{\pm n} + f_{\pm(n+1)}).$$

The entanglement entropy of the block A is (SM)

$$S_A^{\text{scs}} = (\ell + 1)(2 \ln 2 - 1), \quad \ell \leq L, \quad (9)$$

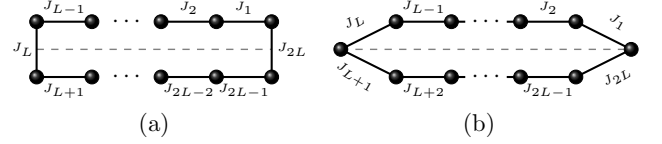


FIG. 1: Illustrating our physical model, Eq. (1) with couplings given in Eq. (3). Symmetrical links with respect to the dashed line carry the same couplings. (a) Bond-centered symmetry (bcs); (b) Site-centered symmetry (scs).

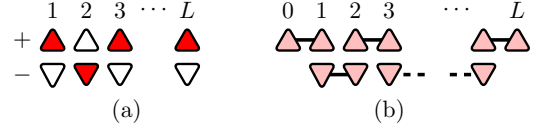


FIG. 2: Ground states of the rainbow XX model in the limit $h \rightarrow \infty$. We use the folded representation of Fig. 1.

which is still linear but not maximal as in Eq.(6).

The long-range entanglement of the bcs/scs states can be converted into short-range one using the basis of states generated by the operators $d_{\pm, n}$ and $f_{\pm, n}$. The d -operators are the bonding and anti-bonding combinations of the fermions located at opposite sites in the chain. They become local operators by *folding* the chain around the bond $(L, L+1)$ that transforms it into a ladder with 2 legs and L rungs. The folding *trick* has played an important role in the study of quantum impurity problems [39–41]. Equation (4) shows that the bcs state is the product of bonding and antibonding states on the rungs. Hence, the entanglement entropy of the block $C = \{L+1-\ell, \dots, L+\ell\}$ located at the center of the chain, that corresponds to ℓ rungs in the ladder, is simply

$$S_C^{\text{bcs}} = 0, \quad \ell = 1, \dots, L-1. \quad (10)$$

Turning to the site-centered chains we observe that the f -operators, Eq. (8), involve a folding transformation that leaves sites 1 and $L+1$ untouched. The chain is now transformed into a ladder with $L-1$ rungs and two isolated sites on both edges. The entanglement entropy of block $C = \{L+2-\ell, \dots, L+\ell\}$ located at the center of the chain (see Fig. 1), that corresponds to ℓ rungs in the ladder and one site, is given by

$$S_C^{\text{scs}} = \ln 2, \quad \ell = 1, \dots, L-1. \quad (11)$$

One can verify Eqs.(10) and (11) by looking at Fig. 2 which shows that the GS of the bcs rainbow is a charge density wave (CDW), while that for the scs rainbow is a staggered dimer state, reminiscent of the trivial and topological phases of the well known SSH model [42]. The origin of these GS structures can be understood writing

the Hamiltonian Eq. (1) using the operators (5) and (8),

$$\begin{aligned}
H_{\text{bcs}} &= -\frac{1}{2} \left[\sum_{n=1}^{L-1} J_{L-n} (d_{+n}^\dagger d_{+n+1} + d_{-n}^\dagger d_{-n+1}) \right. \\
&\quad \left. + J_L (d_{+1}^\dagger d_{+1} - d_{-1}^\dagger d_{-1}) \right. \\
&\quad \left. + J_{2L} (d_{+L}^\dagger d_{+L} - d_{-L}^\dagger d_{-L}) + \text{h.c.} \right], \\
H_{\text{scs}} &= -\frac{1}{2} \left[\sum_{n=1}^{L-2} J_{L-n} (f_{+n}^\dagger f_{+n+1} + f_{-n}^\dagger f_{-n+1}) \right. \\
&\quad \left. + \sqrt{2} J_L f_0^\dagger f_{+1} + \sqrt{2} J_1 f_L^\dagger f_{+L-1} + \text{h.c.} \right]. \quad (12)
\end{aligned}$$

In the bcs model the chemical potential on the first rung induces, in the strong inhomogeneity limit, the full occupation of site +1 and the emptying of site -1. This mechanism gives rise to a CDW state. In the scs model, the hopping term between the isolated mode f_0 and the mode f_{+1} of the first rung, induces in the same limit, a hybridization that propagates along the chain producing a staggered dimer state on the ladder. These ground states are illustrated in Fig. 2. The bcs state is a product state in the basis $d_{\pm,n}$, so a MPS with bond dimension $\chi = 1$. On the other hand, the scs state is a product of dimers, with bond dimension $\chi = 2$ (SM). The entanglement spectrum is twofold degenerate with two equal eigenvalues. We shall next show that the previous topological features persist for all values of $h > 0$. Fig. 3 shows the entanglement entropies (EE) of the central blocks $A = [-x, x]$ for the bcs and scs rainbows. They are independent of x , for sufficiently large values, so corresponding to an area law for the folded chain. Notice that when $h \gg 1$ the EE for the bcs chains goes to zero while that for the scs chains goes to $\ln 2$, in agreement with Eqs. (10) and (11). The rainbow chain has a continuum limit given by a massless Dirac fermion on a curved spacetime. Using CFT techniques one can find the entanglement entropy of the central block [32] $A = [-x, x]$ (with $x = n - L - \frac{1}{2}$ for bcs chains and $x = n - L - 1$ for the scs chain) is

$$S_C(x) \simeq \frac{1}{3} \ln \left[\frac{4\tilde{L}}{\pi} e^{-hx} \sin \frac{\pi\tilde{x}}{\tilde{L}} \right] + E_1 < \frac{1}{3} \ln \frac{4}{h} + E_1 \quad (13)$$

where $\tilde{x} = (e^{hx} - 1)/h$ and $E_1 \simeq 0.49502$. Fig.3 shows that this expression reproduces the bcs and scs entropies when h is not too large, where the field theory limit applies. The upper bound in Eq.(13) is similar to the EE of a massive theory in the scaling limit with $1/h$ as correlation length [31].

Another signature of a SPT phase is the degeneracy of the entanglement spectrum (ES) [8, 11]. For a free fermion system the entanglement energies are given by $E(\{n_p\}) = \sum_p \varepsilon_p n_p + r_0$, where $\{n_p = 0, 1\}$ is the set of occupation numbers of the one-body entanglement entropies ε_p that are computed from the eigenvalues of the

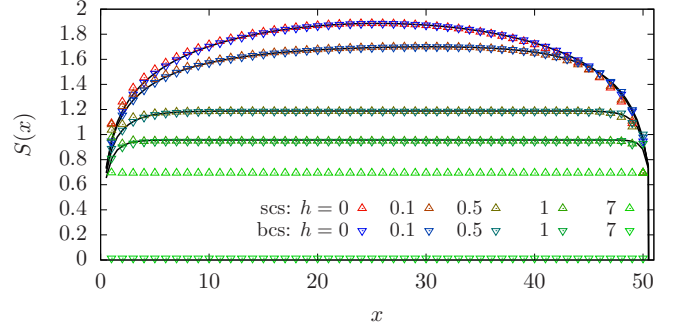


FIG. 3: Entanglement entropy of the central block for increasing values of h shown in descending order, of the bcs and scs chains with $L = 51$. The continuum lines are the CFT prediction (13).

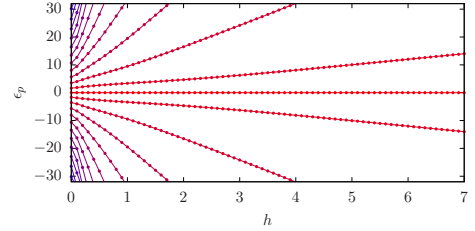


FIG. 4: Single particle entanglement spectrum ε_p for a scs chain with $L = 51$ as a function of h .

correlation matrix $\langle c_n^\dagger c_m \rangle$ [43]. For scs chains there exists a zero mode, $\varepsilon_0 = 0$, for all values of h , that gives rise to a doubly degeneracy of the ES (see Fig. 4). This degeneracy is protected by the time reversal and particle-hole symmetry of the Hamiltonian. Hence, this model belongs to the symmetry class BDI of topological invariants for free fermions, the same as the SSH model [10, 18, 42]: a perturbation to the Hamiltonian that does not respect those symmetries will break the ES degeneracy.

The rainbow antiferromagnetic Heisenberg model.- The Hamiltonian is

$$H = \sum_{n=1}^{2L} J_n \mathbf{S}_n \cdot \mathbf{S}_{n+1}, \quad (14)$$

where \mathbf{S}_n are the spin 1/2 matrices at site n . The couplings J_n are defined in Eq. (3). Let us study the phases of this model in the limit $h \gg 1$. For the bcs chain, the analysis is similar to the one of the bcs XX chain. The Dasgupta-Ma RG equation yields a GS made of spin singlets between sites n and $2L + 1 - n$. Folding the chain maps this state into the product of L rung singlets of the two leg ladder. In the scs chain, the highest couplings are $J_L = J_{L+1}$, and we start diagonalizing the Hamiltonian $J_L \mathbf{S}_{L+1} \cdot (\mathbf{S}_L + \mathbf{S}_{L+2})$. Its GS is obtained by forming a triplet between spins \mathbf{S}_L and \mathbf{S}_{L+2} , that couples to spin \mathbf{S}_{L+1} yielding an effective spin 1/2, denoted as \mathbf{S}'_{L+1} . First order perturbation theory yields the RG equations $\mathbf{S}_L, \mathbf{S}_{L+2} \rightarrow \frac{2}{3} \mathbf{S}'_{L+1}$. The next order term

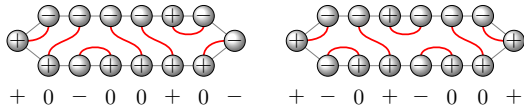


FIG. 5: Strong inhomogeneity limit of the GS of the scs Heisenberg model. The links represent valence bonds. The \pm symbols inside the balls denote the sign of σ^z of the corresponding spin, while the sign of the sum over the rung appears below. These signs display an antiferromagnetic liquid behaviour characteristic of the Haldane phase.

in the Hamiltonian is $J_{L-1}(\mathbf{S}_{L-1} \cdot \mathbf{S}_L + \mathbf{S}_{L+2} \cdot \mathbf{S}_{L+3})$ that gets renormalized into $\frac{2}{3}J_{L-1}\mathbf{S}'_{L+1} \cdot (\mathbf{S}_{L-1} + \mathbf{S}_{L+3})$, so we can repeat the same RG step done above if $h \gg 1$. Each RG step generates an effective spin 1 that couples to an effective spin 1/2 from the previous step. Completing the RG procedure yields a chain with L effective spins 1 and two spins 1/2 at the ends of the folded chain (see Fig. 5). This is the AKLT [22] state of an open chain with $L-1$ spins 1's and two 1/2's at the ends (SM). The RG method used above is valid for $h \gg 1$, but the topological nature of the GS also holds for all positive values of h . To verify this statement we show in Fig. 6 the string order parameter [25, 44, 46].

$$g(L) = \langle S_1^z e^{i\pi \sum_{j=2}^{L-1} S_j^z} S_L^z \rangle, \quad (15)$$

where $S_j^z = S_{u,j}^z + S_{d,j}^z$ is the spin operator on the j^{th} rung of the folded chain. For bcs chains all rungs are considered, while for scs chains sites 1 and $L+1$ are left out. For the bcs chains, $|g(L)|$ approaches quickly zero as $h \gg 1$, while for the scs chains $g(L)$ converges asymptotically towards $-4/9$ that corresponds to the AKLT state [25]. Fig. 6-bottom, shows that the EE of the central blocks of the scs model remains constant for sufficiently large values of h , which is a signature of the area law (recall Eq.(13)). The entanglement spectrum is doubly degenerate (see inset of Fig. 6 bottom), that is another feature of the SPT phase, which in this case is protected by the time reversal symmetry [8, 15]. Moreover, if we drop the site $2N$, that is placed in the right most position in Fig. 5, this has the effect of leaving an edge spin of the effective spin 1 chain.

Gapless versus gapped topological phases.— The previous results show that a strong inhomogeneous deformation of the critical spin 1/2 AFH chain, with site centered symmetry, becomes an effective spin 1 chain in the Haldane phase. Let us now consider Heisenberg chains with higher spin. If the spin is a half-odd integer, $S = \frac{1}{2}, \frac{3}{2}, \dots$, then the uniform AFH Hamiltonian is gapless and described by the $SU(2)_1$ WZW model [50]. Applying a strong inhomogeneous scs deformation generates, via its folding, an effective AKLT chain with spin $2S = 1, 3, \dots$. The ground states of these spin chains possess non-trivial SPT phases [15]. Let us now replace the AFH Hamiltonian by the Babujian-Takhtajan (BT)

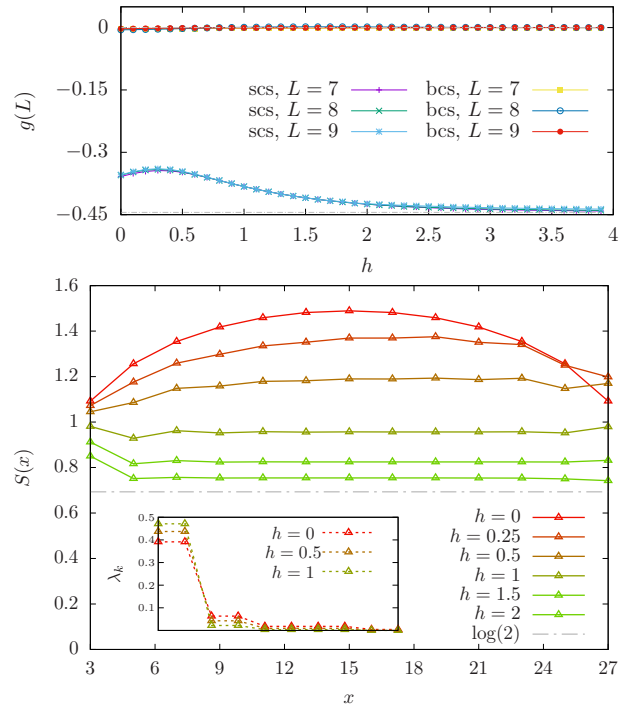


FIG. 6: Top: Plot of the string order parameter, $g(L)$, for the Heisenberg chains with $L = 7, 8, 9$. It vanishes for the bcs chains and approaches the AKLT value $-4/9$ for the scs chains. Bottom: EE of the central blocks of the scs Heisenberg model with $L = 15$ obtained with the DMRG [45] as a function of the size and several values of h . Notice the convergence to $\log 2$ already for $h = 2$. Inset: ES as a function of the order for 3 values of h and central block with $x = 15$ sites.

Hamiltonian [47–49] of spin S that is integrable and described by the $SU(2)_k$ WZW model with $k = 2S$. We also expect its strong scs deformation to map into the AKLT state of spin $2S$. Hence, when k is odd, the AFH and BT models both end up in non-trivial SPT phases. Repeating this process for integer spin chains gives trivial SPT phases. Indeed, the AFH Hamiltonian for integer spin is gapped according to Haldane's conjecture [21]. Its strong scs deformation gives an AKLT state with spin $2S = 2, 4, \dots$ which is a trivial SPT phase integer [15]. The same is expected to hold for the scs deformation of the BT model for integer spin. The difference between even and odd levels of critical spin chains with $SU(2)_k$ symmetry reminds the one based on global anomalies that also lies on the parity of k [20]. The mechanism of relating apparently different phases via inhomogeneities can be extended to other model in 1 and 2 dimensions. An example is the spin 1/2 AFH model on a square lattice. A strong site-centered deformation of the exchange couplings along the X and Y -axes yields a two dimensional AKLT state with spins 2 in the bulk, spins 1 along the edges and spins 1/2 at the corners.

We want also to mention the proposed relation between

SPT phases, boundary CFT and entanglement entropies that was proposed recently in reference [51].

In summary, we have found a new mechanism to generate symmetry protected phases in one dimensional spin chains governed by inhomogeneous local Hamiltonians. The ground states of these models have long range entanglement but folding the chains around their center its becomes short range. We illustrate this method with the spin $1/2$ XX and antiferromagnetic Heisenberg chains whose inhomogeneous deformations, with site-centered symmetry, yields ground states in the SSH and Haldane phases respectively. We expect this mechanism to work for other 1D and 2D models, that poses the question of which SPT and topological phases can be constructed playing this *origami* game, and whether they could be realized experimentally for example by applying pressure to real materials, or in synthetic materials realized in optical lattices [52].

Acknowledgements.

We would like to thank V. Alba, I. Bloch, P. Calabrese, X. Chen, J. I. Cirac, A. Feiguin, E. Kim, J. I. Latorre, E. López, F. Mila, D. Pérez García, G. Ramírez, S. Ryu, E. Tonni and H. Yarloo for conversations. We acknowledge financial support from the grants FIS2015-69167-C2-1-P, FIS2015-66020-C2-1-P, QUITEMAD+ S2013/ICE-2801 and SEV-2016-0597 of the “Centro de Excelencia Severo Ochoa” Programme.

-
- [1] D.C. Tsui, H.L. Stormer and A.C. Gossard, Two-dimensional magnetotransport in the extreme quantum limit, *Phys. Rev. Lett.* **48**, 1559 (1982).
 - [2] B.A. Bernevig and T. L. Hughes, *Topological insulators and Topological superconductors*, Princeton Univ. Press (2013)
 - [3] B. Yan and C. Felser, *Topological Materials: Weyl Semimetals*, *Ann. Rev. Cond. Matt Physics*, Vol. 8:337-354 (2017)
 - [4] X.-G. Wen, Vacuum degeneracy of chiral spin states in compactified space, *Phys. Rev. B* **40**, 7387 (1989).
 - [5] T. Kennedy and H. Tasaki, Hidden symmetry breaking and the haldane phase in $s = 1$ quantum spin chains, *Comm. math. physics* **147**, 431484 (1992).
 - [6] A. Altland and M. R. Zirnbauer, Nonstandard symmetry classes in mesoscopic normal-superconducting hybrid structures, *Phys. Rev. B* **55**, 1142 (1997).
 - [7] Z.-C. Gu and X.-G. Wen, Tensor-entanglement-filtering renormalization approach and symmetry protected topological order, *Phys. Rev. B* **80**, 155131 (2009).
 - [8] F. Pollmann, E. Berg, A.M. Turner and M. Oshikawa, Entanglement spectrum of a topological phase in one dimension, *Phys. Rev. B* **81**, 064439 (2010).
 - [9] L. Fidkowski, Entanglement Spectrum of Topological Insulators and Superconductors, *Phys. Rev. Lett.* **104**, 130502 (2010).
 - [10] L. Fidkowski and A. Kitaev, Topological phases of fermions in one dimension, *Phys. Rev. B* **83**, 075103 (2011).
 - [11] A. M. Turner, F. Pollmann and E. Berg, Topological phases of one-dimensional fermions: An entanglement point of view, *Phys. Rev. B* **83**, 075102 (2011).
 - [12] N. Schuch, D. Pérez-García and I. Cirac, Classifying quantum phases using matrix product states and projected entangled pair states, *Phys. Rev. B* **84**, 165139 (2011).
 - [13] X. Chen, Z.-C. Gu and X.-G. Wen, Classification of Gapped Symmetric Phases in 1D Spin Systems, *Phys. Rev. B* **83**, 035107 (2011).
 - [14] X. Chen, Z.-C. Gu and X.-G. Wen, Complete classification of 1D gapped quantum phases in interacting spin systems, *Phys. Rev. B* **84**, 235128 (2011).
 - [15] F. Pollmann, E. Berg, A.M. Turner and M. Oshikawa, Symmetry protection of topological order in one-dimensional quantum spin systems, *Phys. Rev. B* **85**, 075125 (2012).
 - [16] X. Chen, Z.-C. Gu, Z.-X. Liu, and X.-G. Wen, Symmetry protected topological orders and the group cohomology of their symmetry group, *Phys. Rev. B* **87**, 155114 (2013).
 - [17] L. Tsui, F. Wang and D.-H. Lee, Topological versus Landau-like phase transitions, arXiv:1511.07460 (2015).
 - [18] A. Bernevig and T. Neupert, Topological Superconductors and Category Theory, arXiv:1506.05805 (2015).
 - [19] G. Y. Cho, K. Shiozaki, S. Ryu and A.W.W. Ludwig, Relationship between Symmetry Protected Topological Phases and Boundary Conformal Field Theories via the Entanglement Spectrum, *J. Phys. A: Math. Theor.* **50**, 304002 (2017).
 - [20] S.C. Furuya and M. Oshikawa, Symmetry protection of critical phases and a global anomaly in $1 + 1$ dimensions, *Phys. Rev. Lett.* **118**, 021601 (2017).
 - [21] F. D. M. Haldane, Nonlinear Field Theory of Large-Spin Heisenberg Antiferromagnets: Semiclassically Quantized Solitons of the One-Dimensional Easy-Axis Nél State, *Phys. Rev. Lett.* **50**, 1153 (1983).
 - [22] I. Affleck, T. Kennedy, E.H. Lieb and H. Tasaki, *Commun. Math. Phys.* **115**, 477 (1988).
 - [23] U. Schollwoeck, The density-matrix renormalization group in the age of matrix product states, *Ann. Phys.* **326**, 96-192 (2011).
 - [24] R. Orús, A practical introduction to tensor networks: Matrix product states and projected entangled pair states, *Ann. Phys.* **349**, 117-158 (2014).
 - [25] M. den Nijs and K. Rommelse, Preroughening transitions in crystal surfaces and valence-bond phases in quantum spin chains, *Phys. Rev. B* **40**, 4709 (1989).
 - [26] J. Haegeman, D. Pérez-García, I. Cirac and N. Schuch, Order Parameter for Symmetry-Protected Phases in One Dimension, *Phys. Rev. Lett.* **109**, 050402 (2012).
 - [27] M. B. Hastings, Solving gapped Hamiltonians locally, *Phys. Rev. B* **73**, 085115 (2006).
 - [28] M. M. Wolf, F. Verstraete, M. B. Hastings, and I. Cirac, *Phys. Rev. Lett.* **100**, 070502 (2008).
 - [29] G. Vitagliano, A. Riera, and J. I. Latorre, Volume-law scaling for the entanglement entropy in spin $1/2$ chains, *New J. Phys.* **12**, 113049 (2010).
 - [30] G. Vidal, J. I. Latorre, E. Rico, and A. Kitaev, Entanglement in Quantum Critical Phenomena, *Phys. Rev. Lett.* **90**, 227902 (2003).
 - [31] P. Calabrese and J. Cardy, Entanglement Entropy and Quantum Field Theory, *J. Stat. Mech.* P06002 (2004).
 - [32] J. Rodríguez-Laguna, J. Dubail, G. Ramírez, P. Cal-

- abrese and G. Sierra, More on the rainbow chain: entanglement, space-time geometry and thermal states, J. Phys. A: Math. Theor. **50**, 164001 (2017).
- [33] E. Tonni, J. Rodríguez-Laguna and G. Sierra, Entanglement hamiltonian and entanglement contour in inhomogeneous 1D critical systems, J. Stat. Mech. 043105 (2018).
- [34] G. Ramírez, J. Rodríguez-Laguna and G. Sierra, From conformal to volume-law for the entanglement entropy in exponentially deformed critical spin 1/2 chains, J. Stat. Mech. P10004 (2014).
- [35] G. Ramírez, J. Rodríguez-Laguna and G. Sierra, Entanglement over the rainbow, J. Stat. Mech. P06002 (2015).
- [36] V. Alba, S. N. Santalla, P. Ruggiero, J. Rodríguez-Laguna, P. Calabrese and G. Sierra, Usual area-law violation in random inhomogeneous systems, to appear in JSTAT. arXiv:1807.04179 (2018).
- [37] C. Dasgupta and S.-K. Ma, Low-temperature properties of the random Heisenberg antiferromagnetic chain, Phys. Rev. B **22**, 1305 (1980).
- [38] D.S. Fisher, Critical behavior of random transverse-field Ising spin chains, Phys. Rev. B **51**, 6411 (1995).
- [39] C.L. Kane and M.P.A. Fisher, Transport in a one-channel Luttinger liquid, Phys. Rev. Lett. **68**, 1220 (1992).
- [40] P. Simon and I. Affleck, Persistent currents through a quantum dot, Phys. Rev. B **64**, 085308 (2001).
- [41] C.A. Busser and A.E. Feiguin, Designing a symmetry protected molecular device, Phys. Rev. B **86**, 165410 (2012);
- [42] W. Su, J. Schrieffer and A. Heeger, Solitons in polyacetylene Phys. Rev. Lett. **42**, 1698 (1979).
- [43] I. Peschel, Calculation of reduced density matrices from correlation functions, J. Phys. A: Math. Gen. **36**, L205 (2003)
- [44] S.M. Girvin and D.P. Arovas, Hidden topological order in integer quantum spin chains, Phys. Scr. **156** (1989).
- [45] S. R. White, Density matrix formulation for quantum renormalization groups, Phys. Rev. Lett. **69**, 2863 (1992).
- [46] S.R. White and D.A. Huse, Numerical renormalization-group study of low-lying eigenstates of the antiferromagnetic $S = 1$ Heisenberg chain, Phys. Rev. B **48**, 3844 (1993).
- [47] L. A. Takhtajan, The picture of low-lying excitations in the isotropic Heisenberg chain of arbitrary spins, Phys. Lett. A **87**, 479 (1982).
- [48] J. Babudjian, Exact solution of the one-dimensional isotropic Heisenberg chain with arbitrary spins S , Phys. Lett. A **90** 479 (1982).
- [49] J. Babudjian, Exact solution of the isotropic Heisenberg chain with arbitrary spins: Thermodynamics of the model, Nucl. Phys. B **215**, 317 (1983).
- [50] I. Affleck and F. D. M. Haldane, Critical theory of quantum spin chains Phys. Rev. B **36**, 5291 (1987)
- [51] G. Y. Cho, K. Shiozaki, S. Ryu and A. W.W. Ludwig, Relationship between Symmetry Protected Topological Phases and Boundary Conformal Field Theories via the Entanglement Spectrum, J. Phys. A: Math. Theor. **50**, 304002 (2017).
- [52] I. Bloch, J. Dalibard, and W. Zwerger, Many-body physics with ultracold gases, Rev. Mod. Phys. **80**, 885 (2008).

SUPPLEMENTAL MATERIALS

XX MODEL

Single-Body Modes

While the bcs chain (see Eq. (1) and Eq. (3)) is tractable via the strong-disorder renormalization group (SDRG) [37, 38], the method is inconclusive for the scs chain. The reason is that there are two hoppings of equal magnitude $\exp(-\frac{h}{2})$. Even if we choose one of them randomly to put a valence bond on it, the degeneracy will propagate to the next renormalization step. Thus, we have developed a different approach via a real space renormalization method à la Wilson, based on the single-particle character of this problem.

Numerical studies of the GS of the scs rainbow system show that the single-body modes are localized in the strong-inhomogeneity limit, but on *four* sites. Moreover, as the modes increase in energy, their support moves outwards from the center of the chain. This leads to a natural renormalization scheme which starts out with the central block, $B^{(1)}$, comprising the three central sites: \bullet_{L-1} , \bullet_L and \bullet_{L+1} . The two internal couplings are the same, equal to $\exp(-h/2)$, so the effective Hamiltonian is:

$$H^{(1)} = -e^{-h/2} \begin{pmatrix} 0 & 1 & 0 \\ 1 & 0 & 1 \\ 0 & 1 & 0 \end{pmatrix}. \quad (16)$$

Its spectrum is composed of three values, E_i , with their associated eigenvectors, $|i^{(1)}\rangle$ where $i \in \{-, 0, +\}$. Let us select the ground state, E_- , which has the form:

$$|{-}^{(1)}\rangle = \frac{1}{2}(1, \sqrt{2}, 1), \quad (17)$$

and keep it as the first electronic orbital. Then we proceed to take the zero mode,

$$|0^{(1)}\rangle = \frac{1}{\sqrt{2}}(1, 0, -1), \quad (18)$$

and take it to the next RG level, along with the orbitals located on the neighboring sites to the block: sites \bullet_{L-2} and \bullet_{L+2} . These three single-body orbitals: $|\bullet_{L-2}\rangle$, $|0^{(1)}\rangle$ and $|\bullet_{L+2}\rangle$ constitute block $B^{(2)}$. Let us build the effective Hamiltonian:

$$H^{(2)} = \begin{pmatrix} \langle \bullet_{L-2} | H | \bullet_{L-2} \rangle & \langle \bullet_{L-2} | H | 0^{(1)} \rangle & \langle \bullet_{L-2} | H | \bullet_{L+2} \rangle \\ \langle 0^{(1)} | H | \bullet_{L-2} \rangle & \langle 0^{(1)} | H | 0^{(1)} \rangle & \langle 0^{(1)} | H | \bullet_{L+2} \rangle \\ \langle \bullet_{L+2} | H | \bullet_{L-2} \rangle & \langle \bullet_{L+2} | H | 0^{(1)} \rangle & \langle \bullet_{L+2} | H | \bullet_{L+2} \rangle \end{pmatrix} \quad (19)$$

The lowest energy eigenstate $|-(2)\rangle$ is kept as a new orbital, and there appears a new zero mode, $|0^{(2)}\rangle = \frac{1}{\sqrt{2}}(1, 0, 1)$, which is taken to the next RG level. The n -th RG step is predicated on a block $B^{(n)}$ which contains the zero mode of the previous step, $|0^{(n-1)}\rangle$ and the next two site-orbitals, $|\bullet_{L-n}\rangle$ and $|\bullet_{L+n}\rangle$, with effective Hamiltonian:

$$H^{(n)} = \begin{pmatrix} \langle \bullet_{L-n} | H | \bullet_{L-n} \rangle & \langle \bullet_{L-n} | H | 0^{(n-1)} \rangle & \langle \bullet_{L-n} | H | \bullet_{L+n} \rangle \\ \langle 0^{(n-1)} | H | \bullet_{L-n} \rangle & \langle 0^{(n-1)} | H | 0^{(n-1)} \rangle & \langle 0^{(n-1)} | H | \bullet_{L+n} \rangle \\ \langle \bullet_{L+n} | H | \bullet_{L-n} \rangle & \langle \bullet_{L+n} | H | 0^{(n-1)} \rangle & \langle \bullet_{L+n} | H | \bullet_{L+n} \rangle \end{pmatrix} \quad n = 1, \dots, L-1 \quad (20)$$

The last step of the procedure is different: the new block is built up with the zero mode of the previous step, but there is only one remaining orbital. Hence, the effective block is a 2×2 matrix:

$$H^{(L)} = \begin{pmatrix} \langle 0^{(L-1)} | H | 0^{(L-1)} \rangle & \langle \bullet_{2L} | H | 0^{(L-1)} \rangle \\ \langle 0^{(L-1)} | H | \bullet_{2L} \rangle & \langle \bullet_{2L} | H | \bullet_{2L} \rangle \end{pmatrix}. \quad (21)$$

$H^{(L)}$ has two different forms depending of nature of last zero mode: if $N \equiv 0 \pmod{4}$, $|0^{(L-1)}\rangle$ is symmetric while if $N \equiv 2 \pmod{4}$ it is antisymmetric. Hence, the energy spectrum presents a double degeneracy of $E = 0$ in the former case, while in the latter it does not.

This RG procedure allows to obtain corrections in h on the step n by choosing the eigenvalue $E_-^{(n)}$. As a consequence of the growth from the center along the RG process, the method can provide corrections to the energy of every single-body mode in subsequent RG steps. Hence, the single-body operator b_1 that appears in the first RG step receives corrections at every RG step. Let us present the single-body modes computed in first order in α . Due to the periodic boundary conditions, the mode b_L^\dagger is, without corrections, the same as b_1^\dagger .

$$\begin{aligned} b_1^\dagger &= \left(\frac{1}{\sqrt{2}} - \frac{e^{-h}}{8\sqrt{2}} \right) c_L^\dagger + \left(\frac{1}{2} - \frac{e^{-h}}{16} \right) (c_{L-1}^\dagger + c_{L+1}^\dagger) + \frac{e^{-\frac{h}{2}}}{\sqrt{2}} \left(\sum_{i=1}^{L-2} \left(\frac{e^{h(2-L+i)}}{\sqrt{2}} \right)^{L-i} (c_i^\dagger + c_{2L-i}^\dagger) + 2 \left(\frac{e^{\frac{L-2}{2}}}{\sqrt{2}} \right)^L c_{2L}^\dagger \right), \\ b_k^\dagger &= \frac{1}{2} \left(c_{L+1-k}^\dagger + c_{L-k}^\dagger + (-1)^{k+1} (c_{L-1+k}^\dagger + c_{L+k}^\dagger) + \sum_{l=1}^{L-2} e^{-\frac{h}{2}l(l+1)} (c_{L-k-i}^\dagger + (-1)^{k+1} c_{L+k+i}^\dagger) \right), \quad k = 2, \dots, L-1, \\ b_L^\dagger &= \frac{1}{2} (c_1^\dagger - c_{2L-1}^\dagger) + \frac{1}{\sqrt{2}} c_{2L}^\dagger, \end{aligned} \quad (22)$$

where c_i^\dagger is the fermionic creation operator on site i . Notice that, due to particle-hole symmetry, each of these modes has a negative energy counterpart. We would like to stress that the physics of the strong coupling can be very well understood by considering zero order on α .

Entanglement Entropy

In this section we derive expression 9 of the entanglement entropy of a block B with l sites of a scs chain. It is well known [43] that the spectrum of the reduced density matrix of fermionic and bosonic lattice systems can be obtained through the diagonalization of the block correlation matrices (CM), C_{ij} :

$$C = \frac{1}{4} \begin{pmatrix} 2 & 1 & 0 & 0 & 0 & 0 & 0 & -1 & 0 & \sqrt{2} \\ 1 & 2 & 1 & 0 & 0 & 0 & 1 & 0 & -1 & 0 \\ 0 & 1 & 2 & 1 & 0 & -1 & 0 & 1 & 0 & 0 \\ 0 & 0 & 0 & 2 & \sqrt{2} & 0 & -1 & 0 & 0 & 0 \\ 0 & 0 & 0 & \sqrt{2} & 2 & \sqrt{2} & 0 & 0 & 0 & 0 \\ 0 & 0 & -1 & 0 & \sqrt{2} & 2 & 1 & 0 & 0 & 0 \\ 0 & 1 & 0 & -1 & 0 & 1 & 2 & 1 & 0 & 0 \\ -1 & 0 & 1 & 0 & 0 & 0 & 1 & 2 & 1 & 0 \\ 0 & -1 & -1 & 0 & 0 & 0 & 0 & 1 & 2 & \sqrt{2} \\ \sqrt{2} & 0 & 0 & 0 & 0 & 0 & 0 & 0 & \sqrt{2} & 2 \end{pmatrix} \quad (24)$$

FIG. 7: Correlation matrix of a $L = 5$ scs chain in the strong coupling limit ($h \rightarrow \infty$) computed via Eq. (23) using the single body modes Eq. (22).

$$C_{ij} = \langle GS | c_i^\dagger c_j | GS \rangle = \sum_{k, k' \in \Omega_{GS}} U_{k,i} \bar{U}_{k',j} \langle GS | b_k^\dagger b_{k'} | GS \rangle = \sum_{k \in \Omega_{GS}} U_{k,i} \bar{U}_{k,j}, \quad (23)$$

where $|GS\rangle$ is the ground state, $U_{k,i}$ is the unitary matrix that diagonalizes the single-body Hamiltonian and Ω_{GS} is the set of the negative single body levels that are occupied. Note that the ground state is degenerate for scs chains with $N \equiv 0 \pmod{4}$, since there is a (double) zero mode in the single-body spectrum. Hence the half-filling is not well defined. In the rest of this section and on the main text we have restricted ourselves to chains with no degeneracy.

The computation of the entropies of the block B requires the diagonalization of the corresponding $l \times l$ block of the CM. In the $h \rightarrow \infty$ limit, when the block B does not include any of the sites $2L, L$ or $L \pm 1$, the submatrix of the CM is tridiagonal and translational invariant (see Fig. 7). The eigenvectors have the following form:

$$|\varphi_k\rangle = \sum_{m=1}^l \phi_m = \sum_{m=1}^l A e^{ikm} + B e^{-ikm}. \quad (25)$$

The eigenvalues are given by:

$$\lambda_k = \frac{1}{2} (1 + \cos k). \quad (26)$$

It is straightforward to obtain the dispersion relation imposing the boundary conditions:

$$\sin(k(l+1)) = 2m\pi \rightarrow k = \frac{2m\pi}{N+1}. \quad (27)$$

The von Neumann entropy is given by:

$$S_{odd}(l) = - \sum_k \lambda_k \log \lambda_k + (1 - \lambda_k) \log (1 - \lambda_k) \quad (28)$$

This finite sum can be evaluated using the Euler-McLaurin formula, inserting a finite width in momentum space, $\Delta_k = \frac{\pi}{l+1}$. We find:

$$S_{scs}(l) = - \frac{l+1}{\pi} \int_0^\pi \left(\cos^2 \frac{k}{2} \log \cos^2 \frac{k}{2} + \sin^2 \frac{k}{2} \log \sin^2 \frac{k}{2} \right) dk = (l+1)(2 \log 2 - 1). \quad (29)$$

The Rényi entropies, defined as

$$S_m = \frac{1}{1-m} \log (\text{Tr} \rho^m), \quad (30)$$

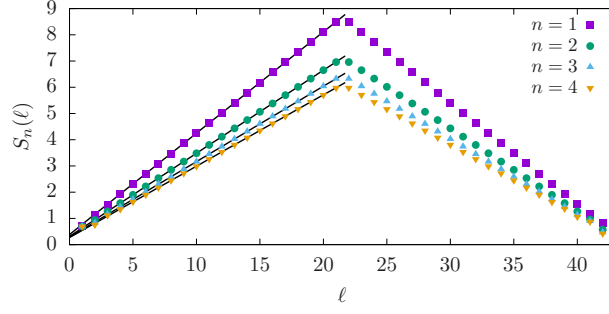


FIG. 8: Different Rényi entropies for a scs system with $L = 21$ and $h = 9.2$. Black lines correspond to the theoretical expressions, Eq. (31).

can also be computed:

$$\begin{aligned}
 S_2(l) &= (l+1) \log(24 - 16\sqrt{2}), \\
 S_3(l) &= (l+1) 2 \log \frac{4}{3}, \\
 S_4(l) &= (l+1) \left(7 \log 2 - \log \left(17 + 8\sqrt{2} + 4\sqrt{26 + 17\sqrt{2}} \right) \right),
 \end{aligned} \tag{31}$$

and these expressions can be seen to match perfectly the numerical data for a scs rainbow chain with $h = 9.2$ and $L = 21$ in Fig. 8.

XXZ INHOMOGENEOUS MODEL.

Hamiltonian

In this appendix we develop an alternative renormalization approach based on the spin formalism which can be extended to the inhomogeneous XXZ model, described by:

$$H = \sum_{n=1}^{2L} J_n \left(S_n^+ S_{n+1}^- + S_n^- S_{n+1}^+ + \frac{\Delta}{2} S_n^z S_{n+1}^z \right) \equiv \sum_{n=1}^{2L} J_n (\mathbf{S}_n \cdot \mathbf{S}_{n+1})_{\Delta} \equiv \sum_{n=1}^{2L} h_n, \tag{32}$$

where J_n follow the rule expressed in Eq. (3). On the regime $h \gg 1$ it is natural to consider only the 3 spins which are coupled with the strongest hopping amplitudes, i.e. $n = L-1, L, L+1$. It can be checked that the GS of this Hamiltonian lies on the sector of the total spin $S_z^{tot} = \frac{1}{2}$, so that it is natural to renormalize the 3 spin block to an effective spin $\frac{1}{2}$, $\mathbf{S}_L^{(1)}$.

$$|\tilde{+}\rangle = \frac{1}{\mathcal{N}} (|++-\rangle - \lambda |+-+\rangle + |-++\rangle), \tag{33}$$

$$|\tilde{-}\rangle = \frac{1}{\mathcal{N}} (-|--+\rangle + \lambda |-+-\rangle - |+- -\rangle), \tag{34}$$

where

$$\mathcal{N} = \sqrt{\lambda^2 + 2}, \quad \lambda = \frac{1}{2}(\Delta + \sqrt{\Delta^2 + 8}), \tag{35}$$

and the GS energy is $E_0 = -\frac{\lambda}{2}$. In order to determine how the spins \mathbf{S}_{L-1} and \mathbf{S}_{L+1} got renormalized we employ the Wigner-Eckhart theorem:

$$\langle \tilde{m} | S_i^a | \tilde{n} \rangle = \xi_i^a \langle \tilde{m} | S_L^{a(1)} | \tilde{n} \rangle, \quad (36)$$

which leads to:

$$\xi_{L-1}^\pm = \xi_{L+1}^\pm = \frac{2\lambda}{\mathcal{N}^2}, \quad \xi_L^\pm = -\frac{2}{\mathcal{N}^2}, \quad (37)$$

$$\xi_{L-1}^z = \xi_{L+1}^z = \frac{\lambda^2}{\mathcal{N}^2}, \quad \xi_L^z = \frac{2 - \lambda^2}{\mathcal{N}^2}. \quad (38)$$

Note that $\sum_n \xi_n^z = 1 \quad \forall \lambda$ and that $\sum_n \xi_n^\pm = \frac{4\lambda-2}{\mathcal{N}^2}$, which is 1 only if the $SU(2)$ symmetry is present. This only holds when $\lambda = 2$, i.e. $\Delta = 1$.

Hence we see that each step of the renormalization involves three spins: s_u and s_d at the edges of the block and one central s_c which is the outcome of each step except the first one, which is physical too (see Fig. 1 (b)).

Fixed Points and RG flow

The next step of the renormalization procedure involves the spins $S_{L\pm 2}$. Using Eq. (38) we notice that the corresponding terms of the Hamiltonian, Eq. (32), can be written in terms of the effective spin of the previous step:

$$e^{-h}((\mathbf{S}_{L-2} \cdot \mathbf{S}_{L-1})_\Delta + (\mathbf{S}_{L+1} \cdot \mathbf{S}_{L+2})_\Delta) = e^{-h}((\mathbf{S}_{L-2} \cdot \mathbf{S}_L^{(1)})_{\Delta'} + (\mathbf{S}_L^{(1)} \cdot \mathbf{S}_{L+2})_{\Delta'}), \quad (39)$$

where

$$\Delta' = \frac{\Delta}{4}(\Delta + \sqrt{8 + \Delta^2}). \quad (40)$$

Imposing $\Delta' = \Delta$, we determine the existence of two fixed points: $\Delta_f = 0$ (XX) and $\Delta_f = 1$ (AFH). Furthermore, iterating this equation while replacing $\Delta \rightarrow \Delta \pm \epsilon$ with $\epsilon \ll 1$ it is straightforward to see that the former is stable ($|\Delta'| < |\Delta|, \Delta < 1$) while the latter is unstable ($\Delta' \geq \Delta, \Delta \geq 1$), as is depicted on Fig. 9.

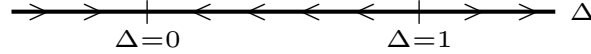


FIG. 9: RG flow in terms of the anisotropy parameter Δ .

MPS form

As it has been described along the RG procedure, each step only considers three spins: two physical ones, s_u, s_d placed on the edges of the block, and an effective spin, s_c placed on the center, which arises from the previous step. These three spins are renormalized into a new effective spin $\frac{1}{2}, s'_c$. Hence, Eq. (34) can be written compactly in the form:

$$|s'_c\rangle = \sum_{s_u, s_c, s_d} A_{s_u s_c s_d}^{s'_c} |s_u s_c s_d\rangle, \quad (41)$$

with

$$A_{sss}^s = A_{ss\bar{s}}^s = \frac{s}{\mathcal{N}}, \quad A_{s\bar{s}s}^s = -\frac{s\lambda}{\mathcal{N}}, \quad s = \pm, \bar{s} = -s. \quad (42)$$

We can rewrite this elementary block of the MPS in another more familiar form where central spins are now indices of the auxiliary space.

$$A_{s_u s_c s_d}^{s'_c} \rightarrow A_{s_c s'_c}^{s_u + s_d}, \quad (43)$$

so that

$$A^- = \frac{\lambda}{\mathcal{N}} \begin{pmatrix} 0 & 0 \\ 1 & 0 \end{pmatrix}, \quad A^+ = \frac{\lambda}{\mathcal{N}} \begin{pmatrix} 0 & -1 \\ 0 & 0 \end{pmatrix}, \quad A^0 = \frac{1}{\mathcal{N}} \begin{pmatrix} 1 & 0 \\ 0 & -1 \end{pmatrix}. \quad (44)$$

If we particularize for the Heisenberg model, we recover (up to an overall constant) the usual matrices that describe the MPS form of the AKLT state [23]. It is straightforward also to build the basis used in [8, 15] to prove the degeneracy of the ES due to the presence of the time reversal symmetry.